Ice Premelting during Differential Scanning Calorimetry

P. W. Wilson,* J. W. Arthur,# and A. D. J. Haymet§
*Physiology Department, School of Medical Sciences, University of Otago, Dunedin, New Zealand; #Institute for Cancer Research, Fox Chase Cancer Center, Philadelphia, Pennsylvania 19111 USA; and §Department of Chemistry and Institute for Molecular Design, University of Houston, Houston, Texas 77204 USA

ABSTRACT Premelting at the surface of ice crystals is caused by factors such as temperature, radius of curvature, and solute composition. When polycrystalline ice samples are warmed from well below the equilibrium melting point, surface melting may begin at temperatures as low as −15°C. However, it has been reported (Bronshteyn and Steponkus, 1993. *Biophys. J.* 65:1853–1865) that when polycrystalline ice was warmed in a differential scanning calorimetry (DSC) pan, melting began at about −50°C, this extreme behavior being attributed to short-range forces. We show that there is no driving force for such premelting, and that for pure water samples in DSC pans curvature effects will cause premelting typically at just a few degrees below the equilibrium melting point. We also show that the rate of warming affects the slope of the DSC baseline and that this might be incorrectly interpreted as an endotherm. The work has consequences for DSC operators who use water as a standard in systems where subfreezing runs are important.

INTRODUCTION

Differential scanning calorimetry (DSC) has been shown to be a valuable tool in studying ice in a variety of biological circumstances (Strambini and Gabellieri, 1996). In this paper we study the DSC of ice formed from pure water, motivated in part by claims (Bronshteyn and Steponkus, 1993, 1994) that solute-free water ice in DSC pans begins to melt at temperatures as low as −50°C. This phenomenon, which might appear to violate basic thermodynamics, was attributed to short-range hydration forces. Below we present evidence which shows that no such melting occurs. Furthermore, we argue that it could not arise from either hydration forces or curvature effects. We show experimentally that melting in pure water begins at −15°C or above, depending on the freezing conditions.

More recently, Bronshteyn and Hopkinson (1996) have quoted results of further DSC studies of glass transition and concentration of freeze-concentrated carbohydrates. Those studies relied heavily on their previous method of DSC baseline calibrations, which assumes that the melting of ice begins at −50°C. We believe it is crucial to examine the accuracy of such baseline calibrations. If premelting and hence endotherms are not to be expected at −50°C, then DSC water-only scans must be examined very closely, and the rate at which warming scans are carried out also must be considered.

In this paper we present results from our own studies of melting of polycrystalline ice in three different DSC instruments, as well as study previously published DSC curves of other workers, where water was used as a control. In addition, we discuss a selection of other premelting results, obtained from experimental methods other than DSC. We discuss the theoretical aspects of ice premelting, especially at the temperature at which liquid water would be expected to exist between polycrystalline ice grain boundaries.

First, we define premelting as the presence of liquid water at the ice surface, or between adjacent ice crystals, at temperatures below the melting point. The level of premelting depends largely on the curvature of the polycrystals of ice, which itself depends on the cooling rate and level of supercooling before the solidification event. The slope of DSC curves during warming is, in some instruments, highly dependent on the warming rate. It is this slope, we believe, that has been misinterpreted as a premelt endotherm. The results and conclusions discussed below are intended to show DSC users that baseline interpretation of the levels of liquid water present must be considered more carefully at the baseline calibration stage. This is especially important in DSC studies on lipids and proteins, where the levels of bound or unfrozen water at subzero temperatures are of interest (Grabielle-Madelmont and Perron, 1983).

EXPERIMENTAL RESULTS

For each of three different DSC instruments, we have taken between 5 and 10 μl of double-distilled water and sealed it in a DSC pan. We then reduced the temperature from ambient to −80°C at 5°C/min, held it at −80°C for 5 min, and then warmed it at either 1°C/min or 5°C/min toward room temperature, while monitoring for any endotherms.

Instrument 1 was a Perkin-Elmer DSC 7, used in the Department of Chemistry at the University of Copenhagen (Denmark). Instrument 2 was a Mettler-Toledo TA 8000, used at the British Antarctic Survey (Cambridge, UK). Instrument 3 was a TA Instruments model TA 2902 modulated DSC, used at the Chemistry Department of the University of Sydney (Sydney, Australia). The results from typical scans from each instrument are shown in Fig. 1. The

---

Received for publication 16 April 1999 and in final form 26 July 1999.

Address reprint requests to Dr. A. D. J. Haymet, Department of Chemistry, University of Houston, Houston, TX 77204. Tel.: 713-743-2781; Fax: 713-743-2709; E-mail: haymet@uh.edu.

0006-3495/99/11/2850/06 $2.00

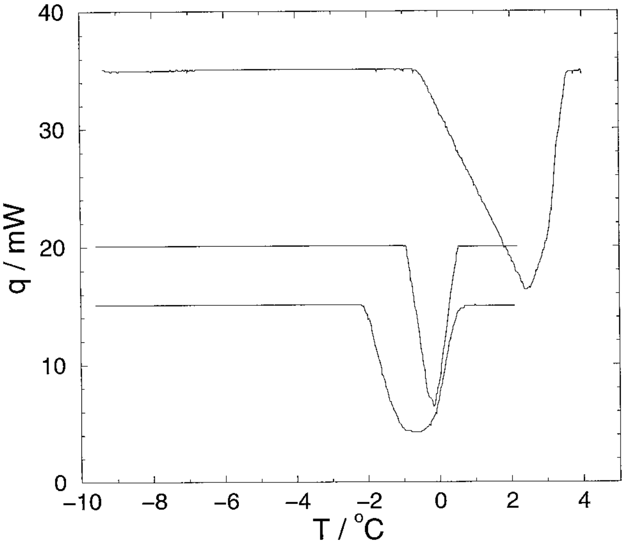

FIGURE 1 Typical warming curves from each of the three DSC devices used to look for premelting endotherms. The bottom trace was produced by the Perkin-Elmer DSC 7 (Department of Chemistry, University of Copenhagen). The middle trace comes from a Mettler-Toledo TA 8000 (British Antarctic Survey, Cambridge, UK). The top trace is from a TA Instruments model TA 2902 modulated DSC (Chemistry Department, University of Sydney, Australia). The scans have been offset for clarity, but the relative heat flows can be directly compared.

areas under the curves, when integrated, indicate different water volumes and do not affect the conclusions we draw below. It can be seen that in all cases no endotherms are visible, and there is no indication of any melting below −3°C.

In Fig. 2 we have reproduced a further two scans from instrument 3. The dashed line shows the data obtained from warming the ice by 5°C/min, and the solid line the data obtained from warming at 1°C/min. On this modulated DSC instrument, where the limit of warming by the machine is claimed to be 5°C/min (TA Instruments manual), when we warmed at that rate a time-temperature lag was observed, and the sample was clearly not at equilibrium. When the sample temperature is out of phase with the instrument as in this case, the problem manifests itself as a slope in the curve and might, mistakenly, be interpreted as an endotherm. However, from examination of the slow warming data, obtained at 1°C/min, we see that the curve is flat and that a slight endotherm, this time due to premelting, starts at approximately −15°C. Note that this is shown as the most expanded vertical scale before noise on the signal significantly affects interpretation of the slope. In Fig. 3 we present the same data as in Fig. 2, but on a less sensitive heat output scale. At this resolution no sign of premelting can be seen.

DISCUSSION

Comparison with previous experiments

In a typical DSC study where water has been used as a control (Grabielle-Madelmont and Perron, 1983), it was found that premelting could not be detected below −2°C. There have also been several studies where water has been confined to restricted geometries during freezing. A typical study (Handa et al., 1992) measured the thermodynamic properties of water by freezing it in silica gels with pore radii in the range of 23–70 Å. It was reported that melting in the pores began at about −20°C in the smallest pores and much closer to 0°C for the larger pores. A similar study (Sartor and Johari, 1996) discussed premelting and pore size and showed that for pores of 85 Å, premelting began at or above −25°C.

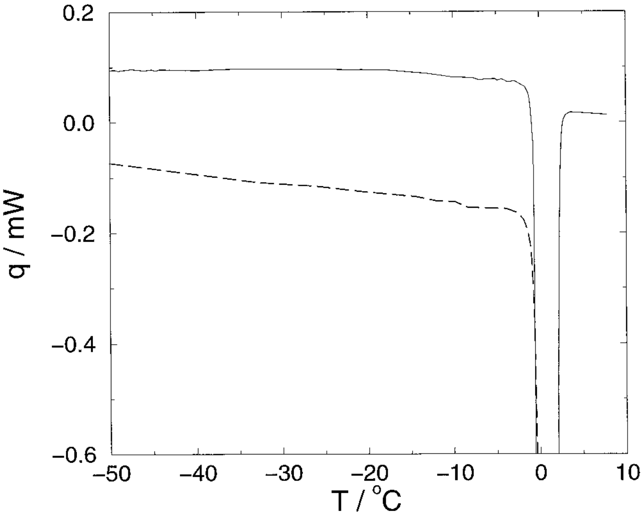

FIGURE 2 Two scans from the same sample, on the modulated DSC TA 2902. – – –, Where the ice was warmed at 5°C/min; ——, where it was warmed at 1°C/min. The slope of the dashed line suggesting premelting is due to the high rate of warming for that machine and the sample being out of equilibrium.

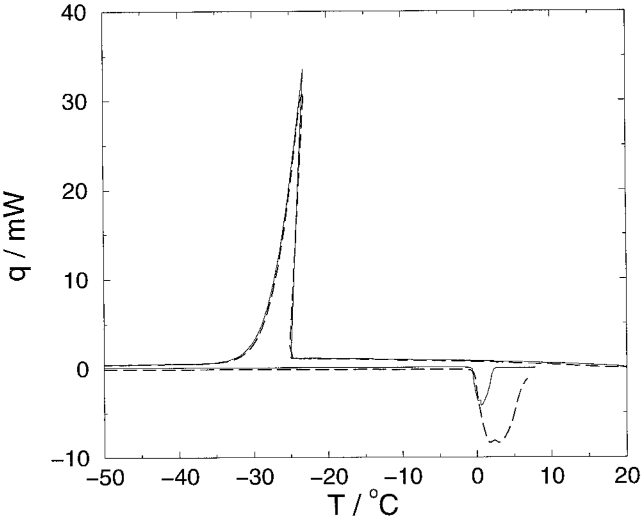

FIGURE 3 The data in Fig. 2 are presented here but on a different scale, and the cooling run has been included. DSC scans such as these, with both endotherms and exotherms shown together, are more commonly published than those shown in Fig. 2. No premelting at all can be seen at this resolution.

In experiments on the freezing of water with added solutes, such as a solution with 73 weight % water (Sartor and Johari, 1996), premelting begins at only −18°C. In a solution of 58% hydroxy ethyl starch (Hansen and Carpenter, 1993), observable premelting begins at approximately −17°C. For a more dilute solution, premelting begins correspondingly closer to 0°C.

In a typical example of DSC usage in biological studies on whole animals, small invertebrates display (Ramløv and Hvidt, 1992) endotherms as low as −30°C. These low-temperature endotherms are attributed to water in the form of aqueous solutions within the animal. Note that these experiments were performed with the DSC 7 instrument that provided the results in the bottom trace of Fig. 1. It is not possible, however, to make direct comparison with such results because of the colligative depression of the melting point and freeze concentration of solutes.

Other types of premelting measurement

There have been several studies of ice premelting where the water has been frozen within powders and gels, many of which were designed to mimic the constriction of water within soils, because it is premelting that is cited as the cause of much-studied frost heaving. In one such study (Maruyama et al., 1992), fine powders were used to increase markedly the surface area in contact with water; the study found liquid water below −20°C. A neutron diffraction study (Gay et al., 1992) of ice grain-boundary melting showed that at −10°C the fraction of the sample that was liquid water was ~0.08 and that no liquid water was measurable below approximately −20°C.

To our knowledge, all such studies show that when the water has been restricted to very small pores, causing the ice crystals to have large curvature, the premelting can be observed at temperatures as low as −30°C. Note, however, that the premelting was not observed with a DSC but with rather more subtle methods. In contrast, a wide-angle x-ray diffraction study where the water was not constricted (Gleeson et al., 1994) found that melting of polycrystalline ice occurs at approximately −5°C. It has been suggested (by an anonymous referee) that NMR measurements may be able to determine the onset of ice premelting. This is an intriguing possibility worthy of expert investigation, but we caution that searching for a water signal in an ice sample at, say −30°C, may not be meaningful; we know of no way to eliminate the possibility of r.f. heating by the NMR field.

We look now at a different type of ice growth assay, a technique called recrystallization inhibition (RI). There are several biological molecules, such as antifreeze proteins (Raymond and DeVries, 1977; Haymet et al., 1999), which are very effective at inhibiting recrystallization of polycrystalline ice at high subzero temperatures. During most recrystallization assays splat cooling of a small droplet of aqueous solution into a polycrystalline ice disc has been used. The discs are then examined on a cryomicroscope at approximately −6°C, and as recrystallization occurs, fewer, larger crystals (or grains) form at the expense of the smaller ones. The effect is directly related to the curvature and surface free energy of each ice grain. Generally, the individual ice crystals have been reported to be within the 1–10-μm-diameter range (Mueller et al., 1991). Note that the water, or solution of interest, is usually quenched at solid CO_2 temperatures (−78°C) and that such deep supercooling gives rise to this size range of crystals. However, in DSC pans, the temperatures of which are lowered at rates usually not exceeding 100°C/min, freezing almost invariably occurs at about −20 to −24°C. Hansen and Carpenter (1993) showed that quenching to −130°C gave crystals on the order of 0.5 μm in diameter. We argue, then, that the ice grains within the DSC pan, which form between −20°C and −30°C, are unlikely to ever be as small as those seen in RI assays. Note, however, that almost always in RI studies the grains have been photographed and hence the size is known, unlike DSC pans, which are sealed closed.

Before recrystallization can occur there must be a thin, surface liquid layer for grain boundary migration, and this is enhanced by either added salt or annealing at −6°C or above (C. A. Knight, personal communication; K. Horwath, personal communication). Between −10°C and −20°C, it has been found that recrystallization drops to a rate that is not measurable, and so this indirectly indicates a minimal liquid layer and therefore minimal (at least not measurable) premelting between grains of the sizes quoted above. Because recrystallization has not been seen below −10°C, cryomicroscopy can be eliminated as a candidate method for testing for ice premelting.

Discussion of previously reported theories

In this section, each of the possible sources of low-temperature premelting will be discussed in turn. These are 1) curvature of ice grain boundaries and the associated Kelvin effect, 2) long-range and short-range hydration forces, 3) dissolved ions, and finally 4) cubic ice formation.

There have been many experimental and theoretical studies of premelting in the ice/vapor system, because of its inherent basic physical interest, especially in climatology. Most studies have concentrated on single, planar ice crystals. One thorough study (Lied et al., 1994a,b) found that premelting at the ice/vapor interface dropped to zero (measurable) from below −10°C to −15°C. However, the Kelvin effect, due to curvature (Wilson, 1993; Reiss et al., 1988), and the interface between ice grains are more relevant to the argument here, because planar crystals are unlikely in a DSC pan and curved, polycrystalline ice will be present. We therefore concentrate our discussion on the ice/ice and the ice/solid interface.

For planar ice surfaces, the ice/water and ice/solid interfaces have been studied by optical techniques including ellipsometry; see, for example, Beaglehole and Wilson (1993, 1994). In summary, it has been found that the ice/

glass interface begins premelting at about −9°C, and roughness and added solutes have a marked effect.

In water-only runs in DSC pans, curvature-induced premelting is the only critical factor, since no impurities are present. We confine further discussion to curvature and the interfacial forces involved. When a DSC pan with, say, 5 μl of water is cooled, it will supercool and freeze at about −25°C into small crystallites, which will have anisotropic crystal symmetry. However, we will assume isotropic ice, with no particular orientation to polycrystals, even though the anisotropy of ice is known to be important in determining premelt behavior on various faces (Beaglehole and Wilson, 1994). With anisotropic solids such as ice, the Hamaker constant is face dependent, but this dependency has no affect on the conclusions we draw below (Dal Corso and Tosatti, 1993), because the onset of premelting does not vary by more than a few degrees between crystal faces.

The liquid water fraction due to the presence of grain boundaries and curvature effects has been discussed in detail by Dash and co-workers (Dash, 1989; Baker and Dash, 1989, 1994; Cahn et al., 1992; Dash et al., 1995). In summary, they show that if the radius of curvature of the ice grains, R, is ~1 μm, a liquid fraction can be present down to about −10°C.

The thickness of any premelt layer is temperature dependent. For dispersion forces (long-range forces) in van der Waals molecules, the theoretical dependence is a power law:

$$d = k(\Delta T)^{n} \tag{1}$$

where $n = 1/3$ and k is a constant. For short-range interactions the growth law describing the liquid thickness is logarithmic (Lowen and Lipowsky, 1991):

$$d = a \ln(\Delta T) \tag{2}$$

where a is a constant, and ΔT is the temperature below the equilibrium melting point in both cases.

It has been argued (Cahn et al., 1992) that van der Waals theory can be used when the thickness d is greater than a few molecular diameters, but that the theory can be readily modified to shorter range forces such as hydration forces. Experimental measurements on a number of van der Waals systems show that there is in fact a logarithmic dependence for thickness at small d, evolving to a power law at larger thicknesses. This can be seen in studies (Gay et al., 1992) of ice grain boundary melting. It was argued that, above about −10°C, dispersion forces should dominate the behavior of the liquid layer. The neutron diffraction data of Gay et al. showed that at −10°C the liquid fraction, f_w, was ~0.08, with none observable below −20°C. Most experimental results have yielded a power law exponent greater than 1/3, and this has been assumed to arise from curvature effects on the ice grains. At temperatures below −10°C, most available data fall below the power law slope, as shown in Fig. 4. This can be explained by a decreased mobility of the melt liquid due to the finite width of the crystal-melt interface (Beaglehole, 1993).

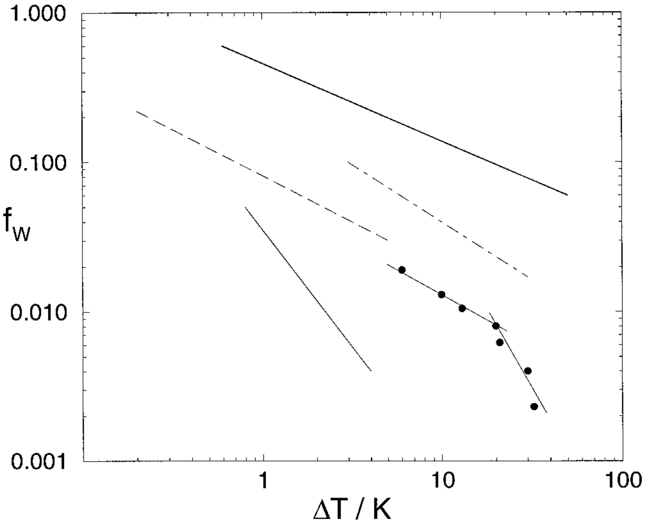

FIGURE 4 This figure shows plots of a variety of experimental data for premelting. The top, solid line indicates the results of the graphite pore work by Gay et al. (1992). The dot-dashed line represents the talc and the dashed line the graphite work of Maruyama et al. (1992). These three have a power law slope close to −0.4. The bottom solid line shows the premelting at the interface between ice and roughened glass in the work of Beaglehole and Wilson (1994). The data points and associated best-fit lines are those of Bronshteyn and Steponkus (1993, 1994). Their shallow section (warmer than −20°C) has a power law slope of very nearly −0.4.

When curvature alone is being considered (Cahn et al., 1992), the radii of curvature cause a freezing point depression,

$$\Delta T = (1/r_1 + 1/r_2) \times 0.0259\ \mathrm{K} \tag{3}$$

where r is measured in μm, leading to 10-Å radii of curvature for a 50°C depression of T_m, a result that is not consistent with what is known about grains in a DSC pan.

The conclusion is clearly that, if premelting is to occur, it cannot be driven by curvature alone. In a detailed look at grain boundary water (Cahn et al., 1992), it was shown that if the radius of curvature is 1 μm or less the liquid fraction is determined by both grain boundaries, curves and crevices between grains. It was calculated that at a grain radius of ~20 μm, short-range forces start to become significant compared to van der Waals forces. In a similar way a summary (Dash, 1989) of Gilpin's regelation data (Gilpin, 1980) showed that the thickness of the liquid layer around a wire imbedded in ice followed the power law with an exponent of 1/3 down to −10°C. Down to this temperature the layer thickness was ~1 nm, after which it dropped to zero and was not measurable below −30°C.

In Fig. 4 we have replotted the results of a variety of premelt studies. It is evident that the data from Bronshteyn and Steponkus (1993) (data points and associated best-fit lines) do not fit the power law with slope 1/3 at temperatures below −20°C. Furthermore, they do not agree with other studies where water was not confined to geometries by graphite or powders.

We look now at short-range forces, and in particular the phenomenon called the hydration force (Attard and Batchelor, 1988). This force is repulsive and is attributed to nonrandom orientation of water molecules within a few molecular layers of a surface (Yan et al., 1993). Water molecules at the boundary between two ice crystals must be oriented toward one or the other of the crystals, because if they were not the crystals would be one, and so some hydration force may exist. It is not clear that such a force will lower the local freezing point, and because only water molecules are present, to come back in line with crystal number two, only a very few layers of water molecules are required to be out of orientation. We argue that a 6–9-Å layer disordered (we resist calling it a liquid layer) between two crystals of radius of at least 5 μm will give $f_w < 0.0004$, insufficient to be detected by even the most sensitive DSC.

When considering the effect of ions on any premelt behavior, one must ask whether premelting could be driven by ions such as H_3O^+ or HCO_3^- (from dissolved CO_2) or OH^-. The discontinuity in the dielectric constants at the ice/water interface (Nada and Furukawa, 1997; Hayward and Haymet, *J. Chem. Phys.*, submitted for publication) is small, and surface ion deficiency is negligible (Beaglehole, 1991). Beaglehole has estimated that at one atmosphere the dissolved CO_2 would depress the melting point by 0.145°C. A recent analysis (Wettlaufer, 1999) reviews impurity effects on ice premelting where ice is in contact with a variety of surfaces. In summary, it has been shown that for premelting below -10°C the thickness of the layer would be less than 1 nm. Because of both of the above findings, we do not further consider ions or impurities as a source of premelting in water-only systems.

A further possible explanation of low-temperature premelting is that at -50°C cubic ice (ice 1c) transforms into hexagonal ice (1h) (Iedema et al., 1998; Lekner, 1998; Johari, 1998a,b). It may be that the endotherm produced during this second-order phase transformation is responsible for the measured baselines (Bronshteyn and Steponkus, 1993). We know of no evidence for the production of cubic ice at -25°C, the typical temperature at which water in a DSC pan freezes.

CONCLUSIONS

In conclusion, there is no driving force for premelting in systems containing only water. During warming, DSC instruments will not detect endotherms caused by a liquid layer between ice grains below -15°C. Furthermore, if the instrument cannot keep up with the rate of warming, the resulting plots will yield a slope that could be interpreted as endothermic and misinterpreted as a premelting event.

Moving beyond our study, we note that Bronshteyn and Steponkus (1993, 1994) claim that the so-called unfreezable water fraction associated with the polar headgroups of lipid bilayers is indeed "freezable," given sufficient time and a low enough temperature. It may be tempting to draw conclusions about water of hydration and bound water based on the levels of premelting measured on a DSC. However, we stress that our results presented above are for samples of pure water only and measure collective behavior. The thermodynamics and kinetics of freezing make determination of the state of a small fraction of water molecules in a biological sample from a nonmolecular technique extremely difficult, and more microscopic spectroscopic techniques seem more appropriate.

We thank Dr. Bill Block of the British Antarctic Survey and Prof. Hans Ramløv of Roskilde University for supplying some DSC scans, use of their instruments, and useful discussions.

In Australia this research was supported by Australian Research Council (ARC) grant A29700122. In the United States this research was supported by ACS-PRF grant 33707-AC9.

REFERENCES

Attard, P., and M. T. Batchelor. 1988. A mechanism for the hydration force demonstrated in a model system. *Chem. Phys. Lett.* 149:206–211.

Baker, M. B., and J. G. Dash. 1989. Charge transfer in thunderstorms and the surface melting of ice. *J. Crystal Growth.* 97:770–776.

Baker, M. B., and J. G. Dash. 1994. Mechanism of charge transfer between colliding ice particles in thunderstorms. *J. Geophys. Res. Atmospheres.* 99:10621–10626.

Beaglehole, D. 1991. Surface melting of small particles, and the effects of surface impurities. *J. Crystal Growth.* 112:663–669.

Beaglehole, D. 1993. Capillary waves on the liquid-vapour interface, and propagation near boundaries. *Physica A.* 200:696–707.

Beaglehole, D., and P. Wilson. 1993. Thickness and anisotropy of the ice water interface. *J. Phys. Chem.* 97:11053–11055.

Beaglehole, D., and P. Wilson. 1994. Extrinsic premelting at the ice glass interface. *J. Phys. Chem.* 98:8096–8100.

Bronshteyn, V. L., and J. Hopkinson. 1996. Measurement of Tg′ and Cg′ by DSC. Abstracts of the 33rd Cryobiology Meeting. 623–624.

Bronshteyn, V. L., and P. L. Steponkus. 1993. Calorimetric studies of freeze-induced dehydration of phospholipids. *Biophys. J.* 65:1853–1865.

Bronshteyn, V. L., and P. L. Steponkus. 1994. Calorimetric studies of freeze induced dehydration of phospholipids. *Biophys. J.* 66:1263.

Cahn, J. W., J. G. Dash, and H. Fu. 1992. Theory of ice premelting in monosized powders. *J. Crystal Growth.* 123:101–108.

Dal Corso, A., and E. Tosatti. 1993. Face-dependent Hamaker constants and surface melting or nonmelting of noncubic crystals. *Phys. Rev. B.* 47:9742–9750.

Dash, J. G. 1989. Surface melting. *Contemp. Phys.* 30:89–100.

Dash, J. G., H. Y. Fu, and J. S. Wettlaufer. 1995. The premelting of ice and its environmental consequences. *Rep. Prog. Phys.* 58:115–167.

Gay, J.-M., J. Suzanne, J. G. Dash, and H. Fu. 1992. Premelting of ice in exfoliated graphite: a neutron diffraction study. *J. Crystal Growth.* 125:33–41.

Gilpin, R. R. 1980. Wire regelation at low temperatures. *J. Colloid Interface Sci.* 77:435–448.

Gleeson, J. T., S. Erramilli, and S. M. Gruner. 1994. Freezing and melting water in lamellar systems. *Biophys. J.* 67:706–712.

Grabielle-Madelmont, C., and R. Perron. 1983. Calorimetric studies on phospholipid-water systems. *J. Colloid Interface Sci.* 95:483–493.

Handa, Y. P., M. Zakrzewski, and C. Fairbridge. 1992. Effect of restricted geometries on the structure and thermodynamic properties of ice. *J. Phys. Chem.* 96:8594–8599.

Hansen, T. N., and J. F. Carpenter. 1993. Calorimetric determination of inhibition of ice crystal growth by antifreeze protein in hydroxyethyl starch solutions. *Biophys. J.* 64:1843–1850.

Haymet, A. D. J., L. G. Ward, and M. M. Harding. 1999. Winter flounder "antifreeze" proteins: synthesis and ice growth inhibition of analogues that probe the relative importance of hydrophobic and hydrogen bonding interactions. *J. Am. Chem. Soc.* 121:941–948.

Iedema, M. J., M. J. Dresser, D. L. Doering, J. B. Rowland, W. P. Hess, A. A. Tsekouras, and J. P. Cowin. 1998. Ferroelectricity in water ice. *J. Phys. Chem. B.* 102:9203–9214.

Johari, G. P. 1998a. On the coexistence of cubic and hexagonal ice between 160 and 240 K. *Philos. Mag. B.* 78:375–383.

Johari, G. P. 1998b. Thermodynamics of water-cubic ice and other liquid-solid coexistence in nanometer-size particles. *J. Chem. Phys.* 109: 1070–1073.

Lekner, J. 1998. Energetics of hydrogen ordering in ice. *Physica B.* 252:149–159.

Lied, A., H. Dosch, and J. H. Bilgram. 1994a. Glancing angle x-ray scattering from single crystal ice surfaces. *Physica B.* 198:92–96.

Lied, A., H. Dosch, and J. H. Bilgram. 1994b. Surface melting of ice I(H) single crystals revealed by glancing angle x-ray scattering. *Phys. Rev. Lett.* 72:3554–3557.

Lowen, H., and R. Lipowsky. 1991. Surface melting away from equilibrium. *Phys. Rev. B.* 43:3507–3513.

Maruyama, M., M. Bienfait, J. G. Dash, and G. Coddens. 1992. Surface melting of ice in graphite and talc powders. *J. Crystal Growth.* 118: 33–36.

Mueller, G. M., R. L. McKown, L. V. Corotto, C. Hague, and G. J. Warren. 1991. Inhibition of recrystallization in ice by chimeric proteins containing antifreeze domains. *J. Biol. Chem.* 266:7339–7344.

Nada, H., and Y. Furukawa. 1997. Anisotropy in molecular-scaled growth kinetics at ice-water interfaces. *J. Phys. Chem. B.* 101:6163–6166.

Ramløv, H., and A. Hvidt. 1992. Artemia cysts at subzero temperatures studied by differential scanning calorimetry. *Cryobiology.* 29:131–137.

Raymond, J. A., and A. L. DeVries. 1977. Adsorption inhibition as a mechanism of freezing resistance in polar fishes. *Proc. Natl. Acad. Sci. USA.* 74:2589–2593.

Reiss, H., P. Mirabel, and R. L. Whetten. 1988. Capillarity theory for the "coexistence" of liquid and solid clusters. *J. Phys. Chem.* 92:7241–7246.

Sartor, G., and G. P. Johari. 1996. Structure relaxation of a vitrified high-protein food, beef, and the phase transformations of its water content. *J. Phys. Chem.* 100:10450–10463.

Strambini, G. B., and E. Gabellieri. 1996. Proteins in frozen solutions: evidence of ice-induced partial unfolding. *Biophys. J.* 70:971–976.

Wettlaufer, J. S. 1999. Impurity effects in the premelting of ice. *Phys. Rev. Lett.* 82:2516–2519.

Wilson, P. W. 1993. Explaining thermal hysteresis by the Kelvin effect. *CryoLetters.* 15:119–126.

Yan, Z. J., J. Pope, and J. Wolfe. 1993. Nuclear magnetic resonance spectroscopy of frozen phosphatidylcholine-D_2O suspensions—a new technique for measuring hydration forces. *J. Chem. Soc. Faraday Trans.* 89:2583–2588.